Polarforschung 80 (3), 127 – 140, 2010 (erschienen 2011)

The Arctic Shelf Regions as a Source of Freshwater and Brine-Enriched Waters as Revealed from Stable Oxygen Isotopes

by Dorothea Bauch[1,2], Jens Hölemann[3], Nils Andersen[4], Elena Dobrotina[5], Anna Nikulina[1,2] and Heidemarie Kassens[1]

Abstract: The water masses of the Arctic Ocean shelf regions are significantly influenced by river water and sea-ice processes. Since river water is highly depleted in $\partial^{18}O$ relative to marine waters as well as to sea-ice, the $\partial^{18}O$ composition and salinity of a water sample can be used to separate the different freshwater water sources. In this paper the distributions of river water, sea-ice melt water or sea-ice formation are discussed for the Kara, Laptev and Beaufort shelves based on $\partial^{18}O$ and salinity data. Depending on the average depth the observed fields of salinity and $\partial^{18}O$ values are different for each region. But comparing the overall $\partial^{18}O$ and salinity correlations reveals a remarkable similarity for these three Arctic shelf regions as similar local bottom-water masses are formed by sea-ice processes. Remnants of these sea-ice derived bottom water masses are found on all shelves during summer at a salinity of about 30.
Investigations at the shelf break of the Kara Sea and Laptev Sea show that river water as well as brine waters are exported to the Arctic Ocean halocline. This export shows inter-annual variability in correlation with wind forcing during summer.

Zusammenfassung: Die Wassermassen der arktischen Schelfregionen sind maßgeblich durch den Eintrag von Flusswasser und Prozessen der Meereisbildung und Schmelze bestimmt. Die $\partial^{18}O$-Signatur und der Salzgehalt des Wassers kann über eine Massenbilanz zur Quantifizierung der verschiedenen Süßwasserquellen genutzt werden, da Flusswasser relativ zu Meerwasser im $\partial^{18}O$-Signal stark abgereichert ist. In dieser Studie wird die räumliche Verteilung von Flusswasser, Meereisschmelzwasser und dem Signal von Meereisbildung in Karasee, Laptewsee und Beaufortsee, basierend auf $\partial^{18}O$- und Salzgehalten diskutiert. In diesen Regionen sind die auftretenden $\partial^{18}O$- und Salzgehalts-Wertebereiche sehr unterschiedlich in Abhängigkeit von den stark unterschiedlichen mittleren Schelftiefen. Dennoch ist jeweils die Korrelation zwischen $\partial^{18}O$-Gehalt und Salzgehalt in allen drei Schelfgebieten bemerkenswert ähnlich. Aus der Korrelation $\partial^{18}O$-Gehalt und Salzgehalt kann auf lokal gebildetes Bodenwasser geschlossen werden, welches durch Meereisbildung geprägt ist. Überreste dieses Bodenwassers sind in allen Schelfgebieten im Sommer bei einem Salzgehalt von etwa 30 identifizierbar. Untersuchungen an der Schelfkante von Karasee und Laptewsee zeigen, dass sowohl Flusswasser als auch durch Meereisbildung geprägtes Bodenwasser in die arktische Salzgehaltsschichtung (Halokline) exportiert werden. Dieser Export variiert jährlich und wird durch den jeweils während der Sommermonate vorherrschenden Windantrieb gesteuert.

[1] IFM-GEOMAR, Wischhofstraße1-3, D-24148 Kiel, Germany; e-mail <dbauch@ifm-geomar.de>
[2] Akademie der Wissenschaften und der Literatur, Geschwister-Scholl-Straße 2, D-55131 Mainz, Germany.
[3] Alfred Wegener Institute for Polar and Marine Research (AWI), Am Handelshafen 12, D-27570 Bremerhaven, Germany.
[4] Leibniz Laboratory, Kiel University, Max-Eyth-Straße 11, D-24118 Kiel, Germany.
[5] Otto-Schmidt-Laboratory for Polar and Marine Research (OSL), 199397 Beringa st. 38, St. Petersburg, Russia.

Manuscript received 07 April 2011, accepted in revised form 13 August 2011.

INTRODUCTION

The Arctic Ocean is a region most sensitive to global climatic processes and changes (e.g. DICKSON 1999). An important part of the Arctic environment is the vast area of continental shelves. While the Arctic Ocean is covered by sea-ice all year, the shelf regions are free of sea-ice during summer. On the shelves river-runoff is introduced and most of the Arctic sea-ice is formed here (AAGAARD & CARMACK 1989); thereby water of a wide range of salinities is supplied to the Arctic Ocean halocline (AAGAARD et al. 1981) and deep and bottom water formation is assumed to occur on the deeper shelf of the Kara Sea (e.g. AAGAARD & CARMACK 1989, BAUCH et al. 1995). The Arctic shelf regions are also important carbon reservoirs (ANDERSON et al. 1998) and planktic $\partial^{13}C$ data indicates that the shelf areas are taking up a significant portion of anthropogenic CO_2 (BAUCH et al. 2000). Understanding the processes and the exchange of water masses between the Arctic Ocean basin and the shelf areas are important in respect to halocline stability. A weaker halocline may impede sea-ice formation and enhance the ocean atmosphere heat flux thereby feeding back positively on Arctic climate warming.

Analysis of the freshwater content and its anomalies in the Laptev and East Siberian seas reveals a considerable freshwater storage and movement between the two areas correlated with atmospheric forcing (DMITRENKO et al. 2008). Observations have shown that the summer atmospheric circulation pattern in the region can strongly influence the contribution of river water to the halocline of the Arctic Ocean (e.g. GUAY et al. 2001, DMITRENKO et al. 2005). In the climatically extreme summer 2007 a significantly different distribution of the sea-ice derived brine signal was observed in the Laptev Sea compared to previous observations in summer 1994. A shift in the distribution of brine waters in the eastern Laptev Sea from the bottom layer to the surface layer altered the salinity range of waters exported into the Arctic Ocean (BAUCH et al. 2009, 2010). If this change in brine water distribution becomes more frequent or persists, it may have long-term consequences on the structure and stability of the Arctic Ocean halocline.

River water is highly depleted in $\partial^{18}O$ relative to marine waters as well as to sea-ice. Therefore the $\partial^{18}O$ composition of the water is a good measure for the amount of river-runoff within the water column. By combining $\partial^{18}O$ and salinity data the fractions of all freshwater sources can be deduced, i.e. river runoff, sea-ice melting or formation. In this paper the freshwater signature of the Arctic shelf regions will be discussed

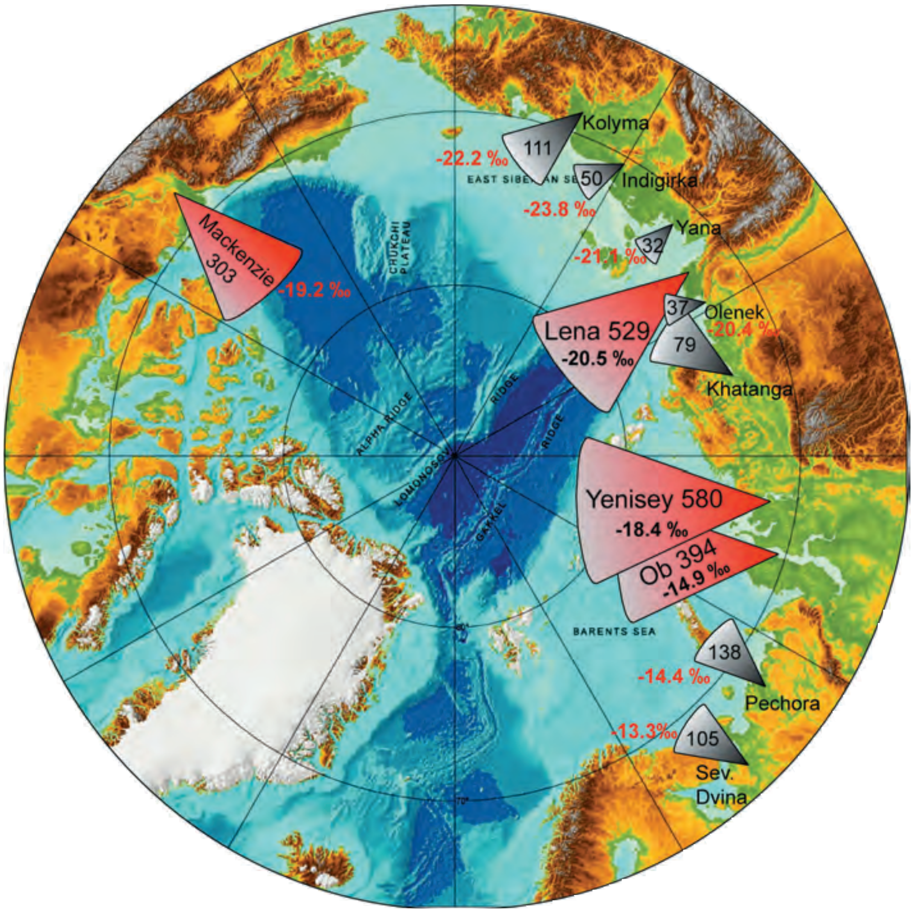

Fig. 1: Geographic map of the Arctic Ocean. Indicated is the mean annual river runoff to the Arctic Ocean in km^3 per year for the 11 largest rivers. The size of each fan represents the amount of runoff in proportion (discharge values from RIMS database). Also indicated are the mean $\partial^{18}O$ values: flow-weighted values for Ob, Yenisey, Lena, Kolyma, Mackenzie rivers (COOPER et al., 2008); summer values for Severnaya Dvina, Pechora, Olenek, Yana, Indigirka (EKWURZEL et al. 2001).

Abb. 1: Geographische Karte des Arktischen Ozeans. Für die elf größten arktischen Flüsse ist der jährliche Gesamtabfluss in km^3 pro Jahr eingetragen und durch die Größe des jeweiligen Fächers repräsentiert (Abflusswerte der RIMS Datenbank). Ebenfalls eingetragen sind die mittleren $\partial^{18}O$-Werte: Abflussgewichtete Werte für Ob, Yenisey, Lena, Kolyma, Mackenzie (COOPER et al. 2008); Sommerwerte für Severnaya Dvina, Pechora, Olenek, Yana, Indigirka nach EKWURZEL et al. (2001).

based on $\partial^{18}O$ and salinity data from the southern and northern Kara Sea, the Laptev Sea and the adjacent continental slopes and from the Beaufort Shelf.

HYDROGRAPHIC SETTING OF THE ARCTIC OCEAN SHELF AREAS

The Arctic shelf areas comprise more than 1/3 of the total Arctic Ocean area. The investigated areas, the Kara, Laptev and Beaufort shelves, all receive huge amounts of river water (Fig. 1) and are seasonally sea-ice covered, but their bathymetries and latitudinal spreading are quite different. The Laptev Sea has an average depth of about 20 m and is the shallowest shelf region. It receives runoff mainly from the Lena River. The southern Kara Sea, with the Yenisey and Ob rivers, has a water depth of about 50 m and smooth topography while the northeastern part is generally deeper including troughs with more than 500 m water depth. The Beaufort Shelf, with the Mackenzie River, is about 50 to 100 m deep and a rather narrow Arctic shelf region. Even though comparable amounts of river water are discharged into each of these regions (Fig. 1) the different topographic settings lead to quite different salinity ranges. The shallowest of the Arctic shelf region, the Laptev Sea, has the lowest salinities measured as the average value from shore to shelf break (see BAUCH 1995, for average salinities of Arctic shelf regions). The average salinity of the southern Kara Sea is slightly higher in correspondence with deeper waters. The Beaufort shelf has the highest salinity, which corresponds with its deeper water depth and its narrow setting. The salinities in the northern Kara Sea are comparable to the values found on the Beaufort shelf.

The shelf regions are free of a permanent sea-ice cover during summer and melt water is released during this time while sea-ice and brine waters are formed during winter. Maximal discharge of Arctic rivers occurs in summer with extremely strong seasonality. For the Lena River the main outflow during June and July is about 4 to 5 times higher than the annual mean discharge of about 529 km^3 a^{-1} (Fig. 1, discharge data taken from the R-ARCTICNET (2011). During winter when the shelves are covered by sea-ice river runoff nearly ceases (e.g. LÉTOLLE et al. 1993).

Due to condensation at low temperatures and successive precipitation over the Eurasian Continent, Arctic river runoff is depleted in stable oxygen isotopes. The Mackenzie River on the Beaufort Shelf has a $\partial^{18}O$ value of about -19 ‰ (COOPER et al. 2008), and is thereby highly depleted relative to marine waters with about 0 ‰ in $\partial^{18}O$. The same is the case for the Siberian rivers also highly depleted in $\partial^{18}O$ that have different freshwater $\partial^{18}O$ values between about -14 to -24 ‰ (Fig. 1). These differences are in accordance with their geographically different drainage areas and successive precipitation from the water vapor moving roughly from west to east across the Eurasian continent (e.g. DANSGAARD 1964; Fig 1) and which is thereby getting progressively depleted in ^{18}O. The $\partial^{18}O$ value of the Kolyma River with about -22 ‰ in the far east of Siberia already reflects the imprint of the Pacific regime and is slightly less depleted compared to the Indigirka with about -24 ‰ slightly further to the west (Fig 1).

MATERIAL AND METHODS

Background information on stable oxygen isotopes and sampling procedure

The most abundant isotope of oxygen is ^{16}O. Further stable oxygen isotopes are ^{17}O and ^{18}O. The natural abundances are 99.76 %, 0.04 % and 0.2 % for ^{16}O, ^{17}O and ^{18}O, respectively. For analysis the ratio of $^{18}O/^{16}O$ (R) is measured and for ocean waters it is given as the permille deviation relative to the standard VSMOW in the usual ∂-notation (CRAIG 1961):
$\partial^{18}O_{sample} = (R_{sample} / R_{standard} - 1) \times 1000$.

Since ^{18}O is heavier a water molecule with $H_2{}^{18}O$ will behave slightly different, e.g. it will evaporate less easy than its lighter counterpart but it will condense earlier than $H_2{}^{16}O$. Therefore there are isotopically different water masses. In the Arctic the isotopic composition of river water (fed by evaporation and successive precipitation of clouds) is most pronounced with a $\partial^{18}O$ value for the Arctic rivers of about -20 ‰, while Atlantic water in the Arctic Ocean has a $\partial^{18}O$ value of about 0.3 ‰ at about 34.92 salinity (BAUCH et al. 1995).

Since $\partial^{18}O$ is measured on the oxygen of the H_2O itself, it is not a trace element and its sampling and conservation is relatively easy (Fig. 2). No poisoning of the water is necessary and some gas-exchange on a short time scale (e.g. bubbling while sampling) is of no harm. Only evaporation has to be prevented and therefore water samples for $\partial^{18}O$ analysis are sampled and stored in glass-bottles closed with caps made from high-density Polyethylen with relatively low permeability for H_2O.

$\partial^{18}O$ and salinity data

Water samples from the Kara Sea (Fig. 3a) were collected during expeditions of RV "Akademik Boris Petrov" in the summers of 1999 (BP99, STEIN & STEPANETS 2000, BAUCH et al. 2003), 2000 (BP00, STEIN & STEPANETS 2001) and 2001 (BP01, STEIN & STEPANETS 2002); for station locations see Fig. 3a). Oxygen isotopes were analyzed at the Leibniz Laboratory (Kiel, Germany) applying the CO_2- water isotope equilibration technique. The measurement precision for $\partial^{18}O$ analysis is ±0.05 ‰, ±0.07 ‰ and ±0.04 ‰ for BP99, BP00 and BP01 samples, respectively.

Fig. 2: Oceanographers prepare for lowering a CTD rosette into the Laptev Sea on board the Russian research vessel "Ivan Petrov" during TRANSDRIFT-XII expedition in 2007. This measuring device collects water samples from different water depths in sample Niskin bottles sealed by remote control. Measurements of conductivity, temperature and pressure are continuously collected by CTD sensors.

Abb. 2: Eine CTD-Rosette wird während der TRANSDRIFT-XII-Expedition im Sommer 2007 auf dem russichen Forschungsschiff "Ivan Petrov" vorbereitet. Dieses Messgerät sammelt Wasserproben in den rosettenförmig angeordneten Niskin-Flaschen, die in unterschiedlichen Wassertiefen elektronisch geschlossen werden. Leitfähigkeit, Temperatur und Druck werden dabei kontinuierlich in der CTD-Messeinheit aufgezeichnet.

Additional salinity and $\partial^{18}O$ data from the southern and northern Kara Sea originates from summer expeditions carried out by the Institute of Water Problems (IVP) in 1976 and 1977 (BREZGUNOV et al. 1980, 1983; Fig. 3a); no information about measurement precision is available.

Water samples from the St. Anna and Voronin troughs located at the Kara Sea shelf break (Fig. 3a) were collected during ARK-XII on board RV "Polarstern" in July 1996. Analysis of $\partial^{18}O$ from this cruise was conducted at the University of Heidelberg, Germany (M. Mensch and M. Frank pers. com.). The measurement precision for $\partial^{18}O$ analysis is ±0.03 ‰.

Salinity and $\partial^{18}O$ data from the Laptev Sea are from expeditions of RV "Prof. Multanovski" in summer 1994 (MÜLLER-LUPP et al. 2003) and RV "Ivan Petrov" during Transdrift Expedition TDXII in summer 2007 (BAUCH et al. 2010; Fig. 3b). Oxygen isotopes were analyzed at the Leibniz Laboratory (Kiel, Germany) applying the CO_2- water isotope equilibration technique. The measurement precision for $\partial^{18}O$ analysis is ±0.07 ‰ and ±0.03 ‰ for data from 1994 and 2007, respectively.

Samples from the Beaufort Shelf were taken in summer 1984 and 1990 (for station locations see Fig. 3c) and salinity and $\partial^{18}O$ data published by ÖSTLUND & GRALL (1993) and MACDONALD et al. (1995), respectively.

Salinity and $\partial^{18}O$ data from the Laptev Sea shelf break are from expeditions of RV "Polarstern" in summers of 1993 and 1995 (FRANK 1996) and analysed at the University of Heidelberg, Germany. Additional samples were collected during NABOS expeditions in September 2005 and 2006 and analyzed at the Stable Isotope Laboratory of the Alfred Wegener Institute (Bremerhaven, Germany) and at the Leibniz Laboratory (Kiel, Germany), respectively. The overall measurement precision for all $\partial^{18}O$ analysis is ±0.03 ‰.

In addition to CTD measurements taken on all expeditions salinity was determined directly within the water samples taken for $\partial^{18}O$ analysis for most stations on the shallow shelf. While all CTD salinity data have a sufficiently high precision, CTD and bottle data on a shallow shelf are sometimes not well matched when aligned by depth due to slight differences in spatial and temporal alignment of the instruments during sampling and due to averaging of the water column at least over the length of each rosette bottle (BAUCH et al. 2010). For a quantitative interpretation of our data an exact match of salinity and $\partial^{18}O$ value is essential. For direct comparison of $\partial^{18}O$ and salinity values, salinity was therefore re-measured directly in the same sample also used for $\partial^{18}O$ analysis. For samples from the southern Kara Sea (BP99, BP00, BP01) these salinity measurements were made using a conductivity meter

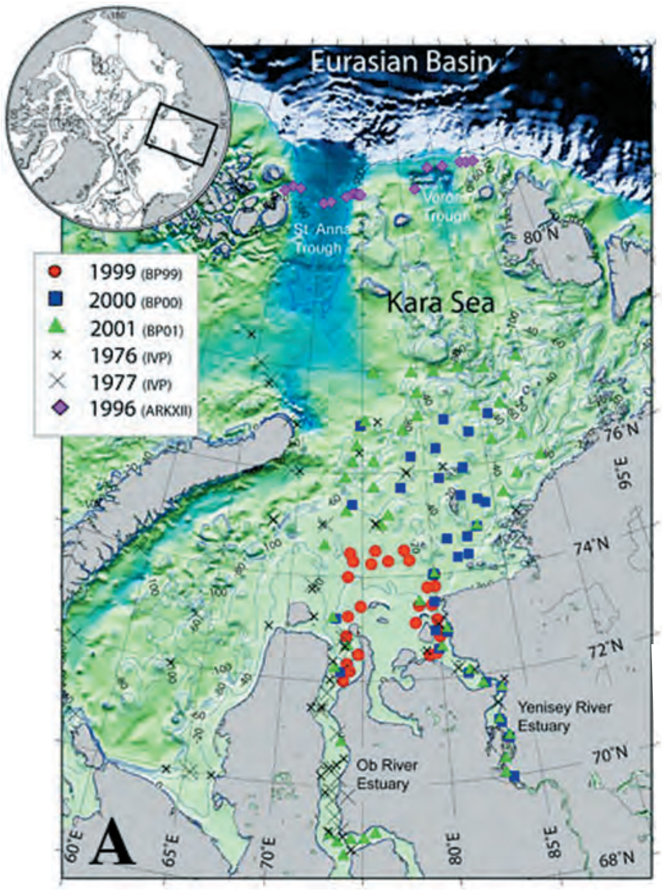

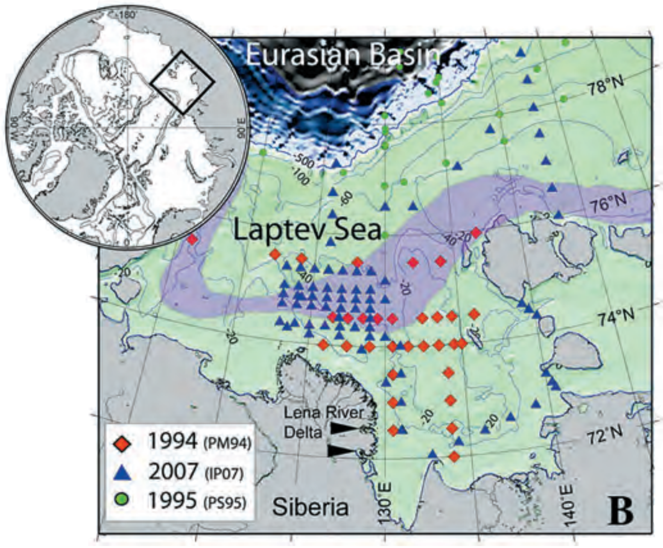

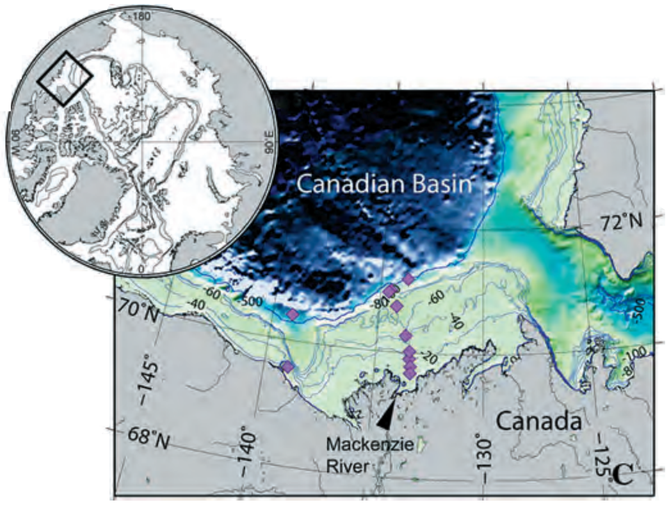

Fig. 3: Geographic position of stations in the Kara Sea (A), Laptev Sea (B) and Beaufort Sea (C). The marked area of index maps shows the position of each shelf area within the Arctic Ocean. The position of the main discharge channels of the Lena River and the Mackenzie River are indicated by black triangles. The shaded purple area in the Laptev Sea (C) indicates the average position of the reoccurring coastal polynya during winter (ZHAKHAROV 1997).

Abb. 3: Geographischen Positionen der Stationen in der Karasee (A), Laptewsee (B) und Beaufortsee (C). Die Lage der Gebiete ist in den jeweiligen Übersichtskarten des Arktischen Ozeans markiert. Die Hauptausstromarme der Lena und des Mackenzie sind durch schwarze Dreiecke markierte. Die violett schattierte Fläche in der Laptewsee (B) zeigt die mittlere Position der wiederkehrenden Küsten-Polynya in der winterlichen Eisbedeckung (ZHAKHAROV 1997).

(LF340/SET from WTW, Weilheim, Germany) with an accuracy of ±0.1 salinity. For the 2007 Laptev Sea samples salinity was determined using an AutoSal 8400A salinometer (Fa. Guildline) with a precision of 0.003 and an accuracy of at least 0.005.

RESULTS

Kara Sea

In the southern Kara Sea and in the Ob and Yenisey estuaries the water column is sharply divided into two vertical layers (Fig. 4). Within the low salinity upper layer there is a strong gradient from the river estuaries to the north, with surface salinities of up to 13 at 74.5 °N (BP99) and up to 28 at 77 °N (BP00). The salinity of the bottom layer increases from about 20 within the estuaries up to 33 at 74.5 °N (BP99) and up to 34.5 at 77 °N (BP00) in the western Kara Sea. In the BP99 dataset the pronounced two-layer structure is extending far to the north, while in the BP00 dataset the water column is considerably less stratified. While the 10 and 20 salinity isolines are found at 10 to 5 m water depth at about 75 °N in the BP99 dataset, they are found at the water surface at about 72.5 °N in the BP00 dataset.

Concurrent with salinity the ∂^{18}O composition shows a similar distribution. All data taken during BP99, BP00, BP01 and the IVP data set have a roughly linear S/∂^{18}O correlation with an average freshwater end member of about -17.0 ‰ (Fig. 5). At low salinities near the river estuaries some regional differences as well as inter-annual differences of about ±1 ‰ (Tab. 1) are apparent. Overall the S/∂^{18}O correlation in bottom layer (Fig. 5) forms two linear lines with a discontinuity at about 30 salinity and about -4 ‰ in ∂^{18}O.

Kara Sea shelf break

Data from the Kara Sea shelf break (RV "Polarstern" ARK-XII) show high salinities (Fig. 6) compared to data sampled at similar depth in the Kara Sea further south (see ranges in Fig. 5 and Fig. 6). Below ~34 salinity the S/∂^{18}O correlation shows

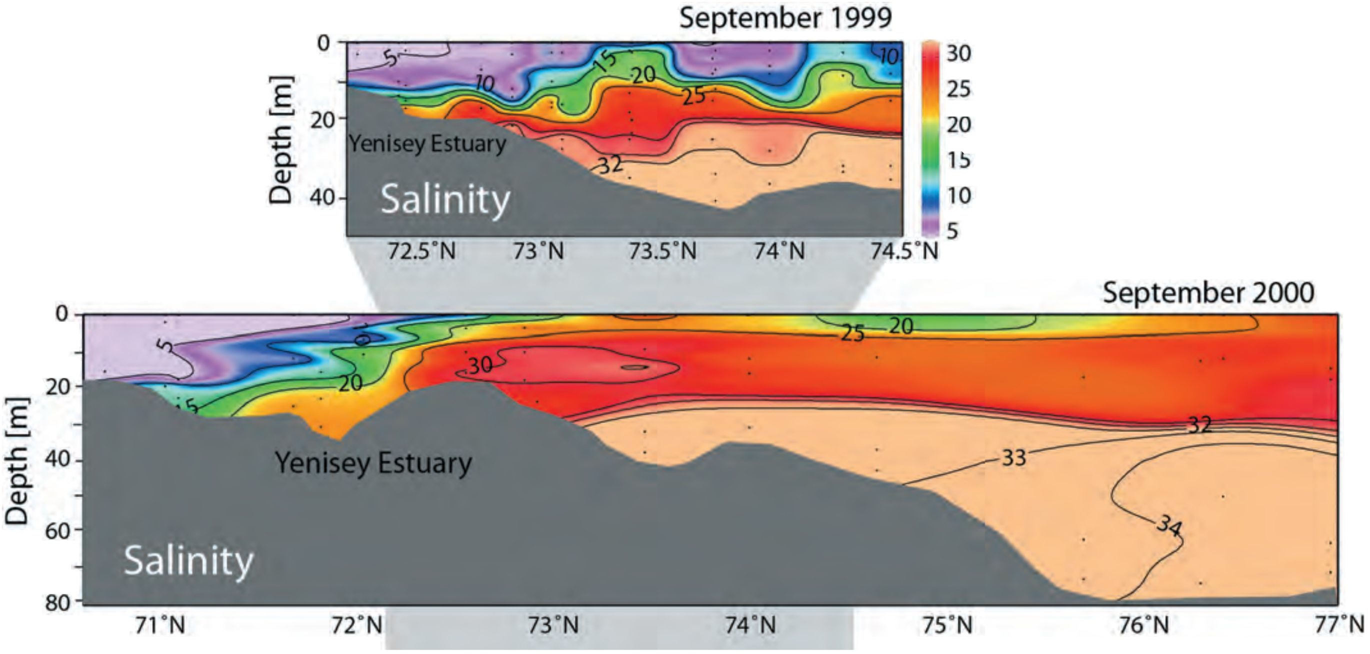

Fig. 4: Salinity data from summer expeditions of RV "Akademic Boris Petrov" to the Kara Sea in September 1999 (BP99) and 2000 (BP00) on sections running from the Yenisey Estuary northwards at about 80 to 85 °E. The dots give position of bottle data and grey shading marks parallel parts of sections.

Abb. 4: Die Salzgehalte in den Sommern 1999 und 2000 in ozeanographischen Schnitten von RV „Akademic Boris Petrov" vom Ästuar des Yenisey nordwärts bei etwa 80 bis 85 °E. Die graue Schattierung markiert den parallelen Teil der Schnitte; die Punkte zeigen die Beprobungstiefen.

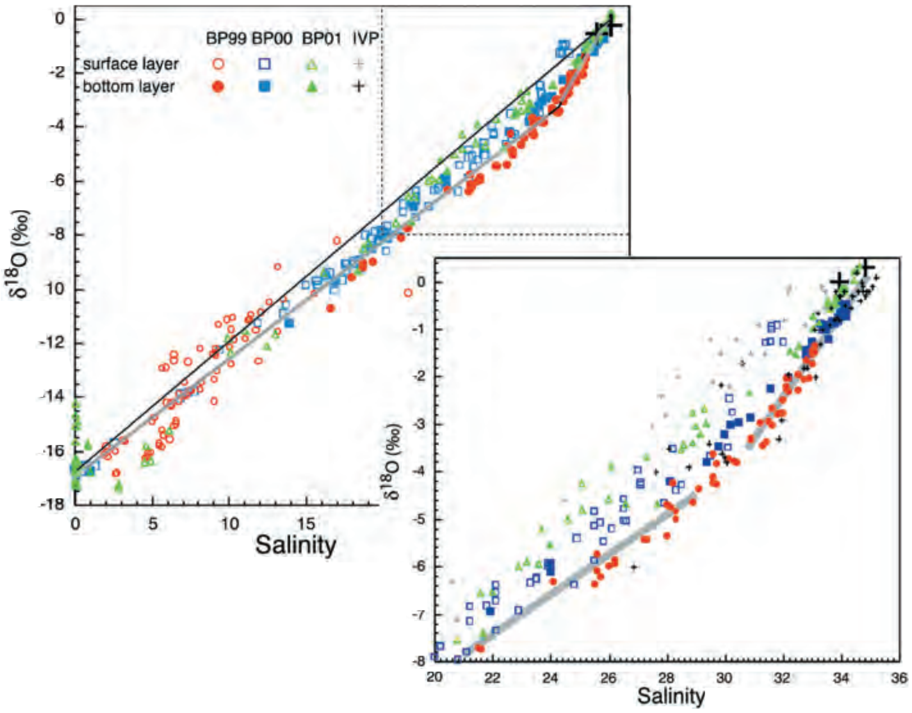

Fig. 5: $\partial^{18}O$ versus salinity for stations in the Kara Sea: circles = BP99, squares = BP00, triangles = BP01. All station data divided by surface layer (open symbols) and bottom layer (closed symbols). The crosses indicate the values of waters entering from the Arctic Ocean and the Barents Sea. The grey lines indicate potential mixing lines, for further explanation see text. The inset (stippled box) shows the same data as enlargement for >20 salinity. In the upper panel the idealized mixing (black line) between river water with -20 ‰ in $\partial^{18}O$ and Atlantic source water with 34.92 salinity and 0.3 ‰ in $\partial^{18}O$ is also indicated for orientation.

Abb. 5: Die $\partial^{18}O$-Werte in Abhängigkeit von den Salzgehalten in der Karasee für die "Akademic Boris Petrov" Expeditionen BP99 = Kreise, BP00 = Quadrate, BP01 = Dreiecke. Für alle Stationsdaten werden Proben aus der Oberflächenschicht (offene Symbole) und der Bodenschicht (gefüllte Symbole) unterschieden. Die Kreuze markieren die Signaturen der einströmenden Wassermassen aus dem Arktischen Ozean und der Barentssee. Die potentiellen Mischungslinien (grau) werden im Text weiter erläutert. Die eingebettet Karte zeigt eine Vergrößerung für Salzgehalte >20. Zur Orientierung ist im oberen Teil ebenfalls die idealisierte Mischungsgerade (schwarze Linie) zwischen reinem Flusswasser (-20 ‰ im $\partial^{18}O$) und reinem "Atlantik Wasser" (Salzgehalt 34.92 und 0.3 ‰ im $\partial^{18}O$) eingetragen.

slight regional differences. But overall the S/$\partial^{18}O$ correlation of the shelf break data fits the correlation of the southern Kara Sea data and blends into the roughly linear correlation of high salinity bottom values.

Laptev Sea

The data from the Laptev Sea resembles the data set from the Kara Sea and also shows strong vertical gradients within the water column (not shown). Also similar to the Kara Sea the spread of low salinity and low $\partial^{18}O$ shows inter-annual variations (Fig. 7). River water remained in both years mostly within the southern Laptev Sea and a predominantly west to east oriented surface salinity front developed within the

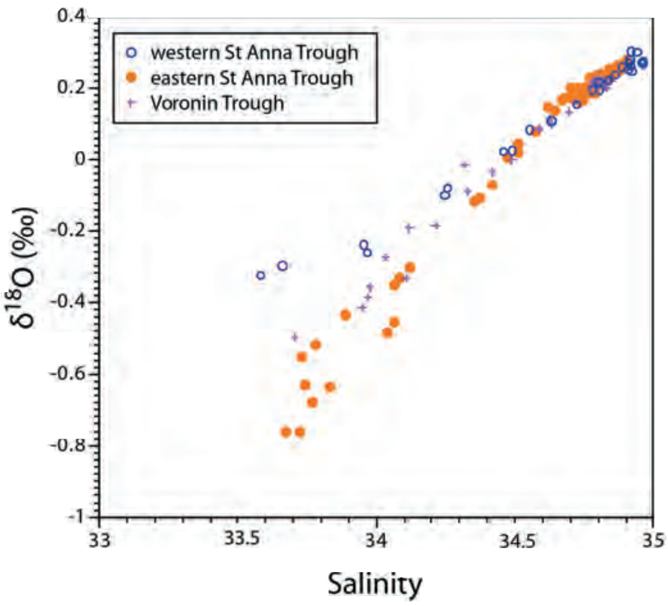

Fig. 6: $\partial^{18}O$ versus salinity for stations from ARK-XII 1996 located along the shelf break of the Kara Sea. Stations are divided by region: western slope of St Anna Trough = open circles, central and eastern slope = closed dots, stations in the vicinity of Voronin Trough = crosses.

Abb. 6: Die $\partial^{18}O$-Werte in Abhängigkeit von den Salzgehalten für Expedition ARK-XII 1996 mit Stationen entlang des Kontinentalhanges der Karasee. Die Stationen sind regional unterteilt in: offene Kreise = westlicher Hang des St. Anna-Grabens, gefüllte Kreise = zentraler und östlicher Hang des St. Anna-Grabens, Kreuze = Umgebung des Voronin-Grabens.

Laptev Sea inner and mid-shelf (Fig. 7) in contrast to years with offshore atmospheric forcing (GUAY et al. 2001) in which a significantly different north to west oriented salinity front prevails within the Laptev Sea (BAUCH et al. 2009). However, river water spread slightly further to the north in 1994, and further towards the east in 2007 (Fig. 7). The $\partial^{18}O$ value of the Lena River is lower compared to the Ob and Yenisey rivers further to the west (Fig. 8). Therefore the general S/$\partial^{18}O$ correlation is similar to that of the Kara Sea, but $\partial^{18}O$ values are lower at low salinities. Similar to the Kara Sea data the Laptev Sea data also shows a discontinuity at roughly 30 salinity for 1994 and ~32 salinity in 2007 (Fig. 8).

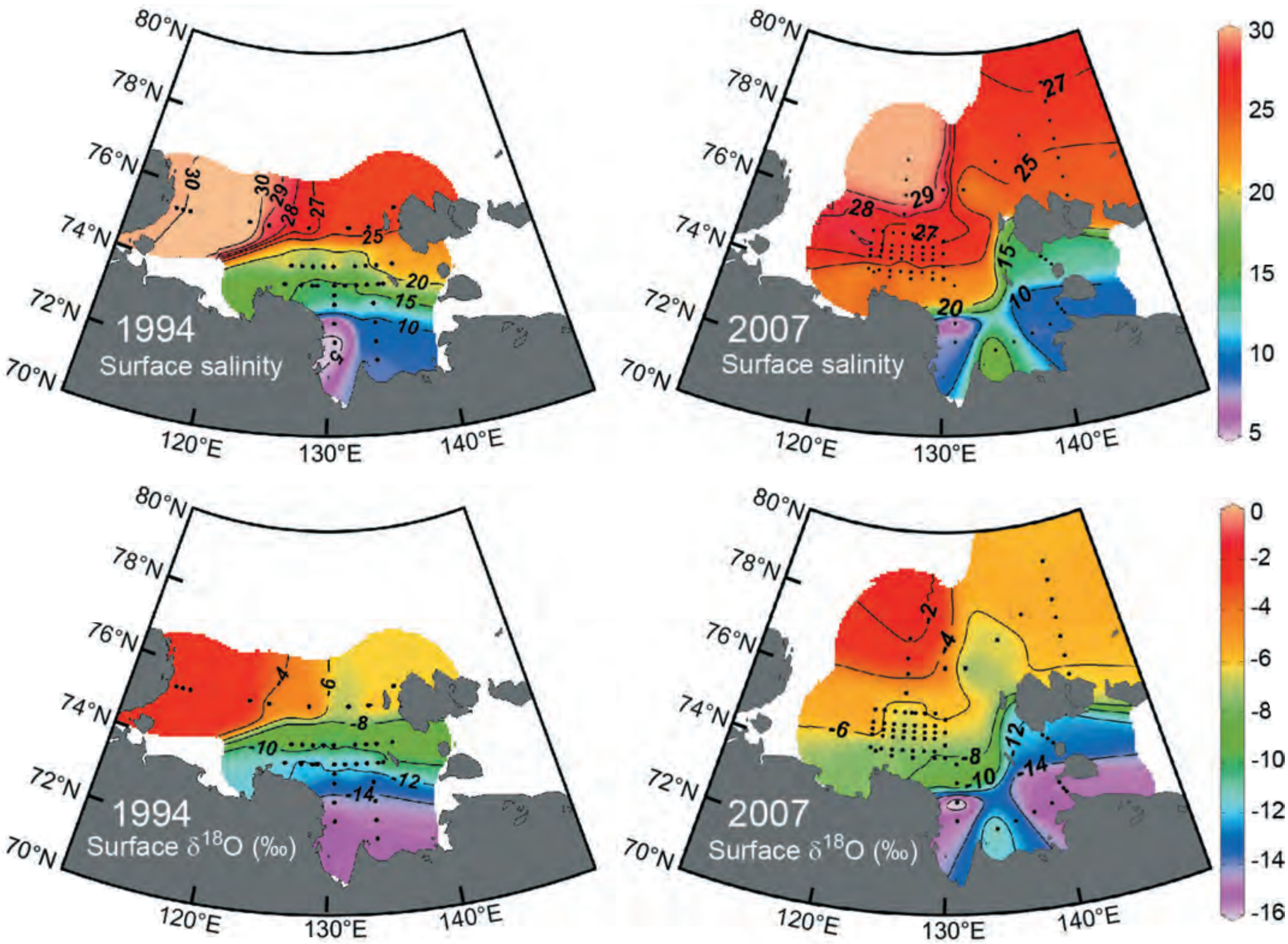

Fig. 7: Surface salinity and surface $\partial^{18}O$ (‰) distribution in the Laptev Sea during summer expeditions in September 1994 (left hand panels) and September 2007 (right hand panels).

Abb. 7: Geographische Verteilung der Salzgehalte und der $\partial^{18}O$ Werte (‰) im Oberflächenwasser der Laptewsee für Sommer 1994 (links) und 2007 (rechts).

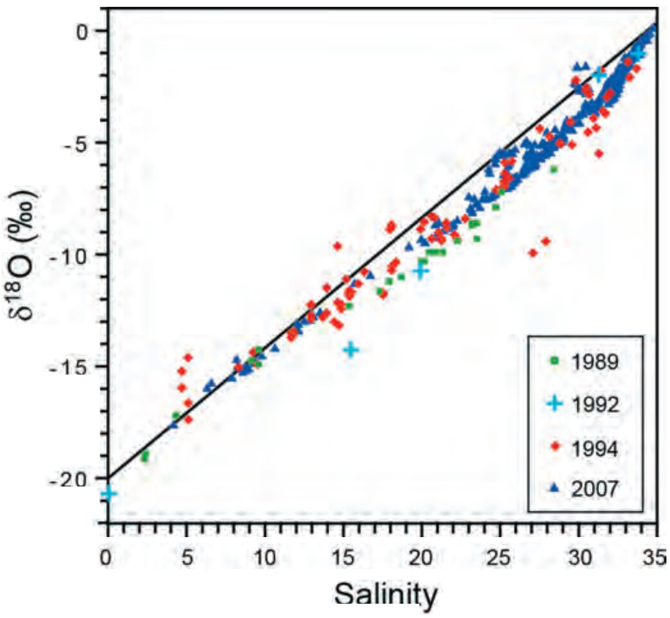

Fig. 8: Property plot of ∂[18]O versus salinity in the Laptev Sea during summers 1994 and 2007 as well as data from the south eastern Laptev Sea from summer 1989 (LETOLLE et al. 1993) and three stations from April 1992 (BAUCH 1995). The line indicates the idealized mixing between river water with -20 ‰ in ∂[18]O and Atlantic source water with 34.92 salinity and 0.3 ‰ in ∂[18]O.

Abb. 8: Die ∂[18]O-Werte in Abhängigkeit vom Salzgehalt in der Laptewsee für Sommerdaten aus dem Jahren 1994 und 2007, ergänzt durch Daten aus der südöstlichen Laptewsee des Sommers 1989 (LETOLLE et al. 1993) und drei Stationen vom April 1992 (BAUCH 1995). Die Gerade repräsentiert eine Mischung zwischen reinem Flusswasser (-20 ‰ im ∂[18]O) und reinem "Atlantik Wasser" (Salzgehalt 34.92 und 0.3 ‰ im ∂[18]O).

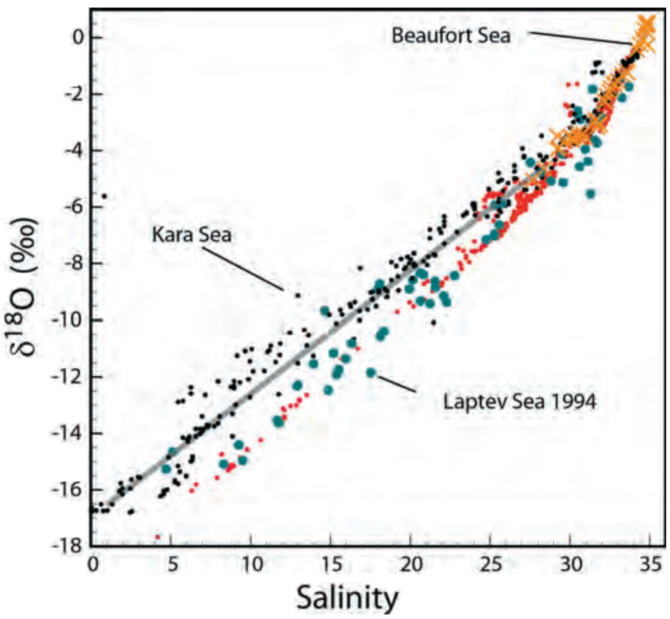

Fig. 9: ∂[18]O versus salinity for stations in the Laptev Sea: blue dots = 1994, red dot = 2007; Beaufort Sea = orange crosses; Kara Sea (BP99, BP00, BP01) = black dots. Mixing lines as also shown in Figure 5 are indicated.

Abb. 9: Die ∂[18]O-Werte in Abhängigkeit von den Salzgehalten in der Laptewsee: blaue Punkte = 1994, rote Punkte = 2007; Beaufort See = orange Kreuze; Karasee (BP99, BP00, BP01) = schwarze Punkte. Mischungslinien wie in Abbildung 5.

Laptev Sea shelf break

Data from the Laptev Sea continental shelf break (RV "Polarstern" 1993 and 1995 and NABOS 2005 and 2006) are close to the marine endmember in ∂[18]O, salinity and have a similar S/∂[18]O correlation (not shown; for positions refer to Fig. 13). Data have typical ranges of ~-3-0.3 in ∂[18]O and ~30-34.95 salinity.

Beaufort shelf

The salinities of waters on the Beaufort shelf are overall higher than those on the Kara and Laptev shelves (Fig. 9). The general S/∂[18]O correlation is however similar to the Kara and Laptev Sea and also indicates a discontinuity at about 30 salinity (Fig. 9).

DISCUSSION

The water structure of all Arctic shelves is governed by inflowing water from the Arctic Basin, continental runoff and sea-ice processes (BAUCH et al. 1995, MACDONALD et al. 1995) and is characterized by an estuarine circulation (MACDONALD 2000, DMITRENKO et al. 2001). This estuarine structure is documented in the vertical structure (see Fig. 4 for Kara Sea sectional data), but stratification might nevertheless be different between years due to the different spread of the summer river plume (see Fig. 6 for Laptev Sea surface data). These differences are caused by general inter-annual variations in atmospheric forcing which determines the surface hydrology in the shallow Laptev Sea (DMITRENKO et al. 2005, SHPAIKHER 1972). Also onshore winds cause a "counter current" at the bottom during summer which transports bottom water from north to south in the Arctic shelf areas as is typical for estuaries. A counter current was detected in mooring results for the Laptev Sea during certain "offshore" atmospheric conditions in summer (DMITRENKO et al. 2001) and described in modeling results for the Kara Sea during summer season, while it was generally absent during autumn (HARMS et al. 1999, 2003).

Variation in ∂[18]O of arctic river water

By linear interpolation of ∂[18]O to zero salinity of inner shelf data the average ∂[18]O value of each river can be determined (Tab. 1). The Ob, Yenisey and Lena rivers have slightly different freshwater ∂[18]O values in accordance with their geographically different drainage areas and successive precipitation from the clouds moving mainly from west to east across the Eurasian continent (e.g. DANSGAARD 1964; see Fig. 1). For the Kara Sea, we have the densest data set covering several years (1976, 1977, 1999-2001). In all these years the isotopic composition of the Yenisey River is about 1 ‰ lighter than that of the Ob River, but absolute values may vary between the years (Tab. 1). Based on these five summer datasets within the river estuaries it can be concluded that inter-annual variation between summer values of the isotopic composition is about 1 ‰ for both the Ob and Yenisey rivers and that there is a constant isotopic difference of about 1 ‰ between these two rivers (BAUCH et al. 2005). It can be further presumed that the strong seasonal variation in discharge volume of each river is

year	season	Ob River δ^{18}O	Yenisey River δ^{18}O	data source
2001	August/September	-15.7 ‰	-17.0 ‰	BAUCH et al. 2005
2000	August/September	-16.1 ‰	-17.0 ‰	BAUCH et al. 2005
1999	August/September	-16.8 ‰	-18.1 ‰	BAUCH et al. 2003
1977	August-October	-15.9 ‰	-18.2 ‰	BREZGUNOV et al. 1983
1977	August-October		-17.0*±0.4 ‰	BREZGUNOV et al. 1983
1977	March	-14.6*±0.5 ‰		BREZGUNOV et al. 1983
1976	August-October	-16.2 ‰	-17.0 ‰	BREZUNOVg et al. 1983
2003-2006	flow-weighted average	-14.9 ‰*	-18.4 ‰*	COOPER et al. 2008

year	season	Lena River δ^{18}O (‰)		data source
1989	September	-19.6 ‰	all stations at about 130°E	LÉTOLLE et al. 1993
1992	April	-20.8 ‰	3 stations only	BAUCH 1995
1994	September	-18.7 ‰		MÜLLER-LUPP et al. 2003
2007	September	-19.8 ‰		BAUCH et al. 2010
2003-2006	flow-weighted average	-20.5‰*		COOPER et al. 2008

Tab. 1: Endmember δ^{18}O values of (top) the Ob and Yenisey rivers derived from linear interpolation of inner estuary data and (bottom) the Lena River interpolated from linear salinity/δ^{18}O correlations from Laptev Sea data south of 75 °N. Additional data based on locally sampled river water are marked with an asterisk.

Tab. 1: Endglieder δ^{18}O Signaturen (oben) des Ob and Yenisey abgeleitet durch lineare Interpolation von Daten aus den inneren Ästuaren und (unten) der Lena abgeleitet durch lineare Interpolation von Salzgehalts/δ^{18}O Daten aus der Laptewsee südlich von 75 °N. Daten basierend auf lokal beprobten Flusswasser sind mit einem Sternchen gekennzeichnet.

also accompanied with seasonal ∂^{18}O changes. COOPER et al. (2008) used seasonal measurements directly within the river to determine flow weighted average ∂^{18}O for the Ob, Yenisey, Lena, and Kolyma rivers as well as for the Yukon, and Mackenzie rivers (see Fig. 1). COOPER at al. found a seasonal variation of ~2 ‰, but no inter-annual variations for the years 2003-2006 (COOPER et al. 2008) in contrast to our results based on interpolation of inner shelf data.

Inter-annual variation in summer ∂^{18}O for the Lena River also indicates about ±1 ‰ (BAUCH et al. 2010; see Tab 1). The inter-annual data from the Laptev Sea has to be interpreted with more caution because only the database for 1994 and 2007 are comparable and have somewhat sufficient coverage.

Both surface and bottom layer of the Arctic shelf regions are the result of mixing between marine water with high ∂^{18}O and riverine water with low ∂^{18}O (Figs. 5, 8 and 9). Relative to the direct mixing line between river and marine water (see black lines in Figs. 5 and 8) all data from the Arctic shelves usually fall below this line at lower ∂^{18}O and/or higher salinities. The deviation of single data points from the direct mixing line is up to 1 ‰ in ∂^{18}O or up to 5 in salinity (see e.g. BP99 data set in Fig. 5) and thus far beyond the analytical uncertainty and documents the admixture of an additional water mass with ~30 salinity and ~-4 ‰ ∂^{18}O. Theoretically also a low ∂^{18}O source might cause the observed deviation, but there is no such process adding a low ∂^{18}O signal without adding an appreciable amount of freshwater as well (as does river water). The only possible explanation is the addition of brine water from sea-ice formation. When ice forms from seawater most of the salt is rejected and resulting brines are injected into the remaining water, while the ∂^{18}O composition of the water is preserved with a small fractionation only (sea-ice was found to be about 2.6 ‰ higher in ∂^{18}O than its source water; MELLING & MOORE 1995). The influence of sea-ice melting and formation is thereby seen in a shift to lower and higher salinities, respectively, at about similar ∂^{18}O. Therefore we can consider the water masses in the Kara, Laptev and Beaufort shelf regions to be a mixture of river water and marine water entering from the Arctic Ocean and also of brine waters produced by net sea-ice formation.

The bottom waters from the Arctic shelf data sets show a systematic division into two separate mixing lines (Fig. 9 and Figs. 5, 8) indicating a distinct water mass at about 30 salinity and -4 ‰ ∂^{18}O. This is most clearly seen for stations taken at about 35 m water depth in the Kara Sea (see BP99 data within Fig. 5, when sampling density was highest in this region). During BP00 and BP01 ∂^{18}O signatures are generally less depleted relative to the direct mixing line between marine and riverine water (see Fig. 5 black line) and a discontinuity in the S/∂^{18}O correlation is observed at slightly higher ∂^{18}O values in both years. Surface data with a salinity range above 30 in the northern Kara and Laptev seas do not exhibit a discontinuity in the S/∂^{18}O correlation as described for the bottom waters. A discontinuity at a salinity of ~30 is also seen within the Kara Sea, the Laptev Sea and the Beaufort Shelf data (Fig. 9). We interpret this discontinuity to reflect the remnant of a water mass formed in winter during enhanced sea-ice formation in flaw polynyas (BAUCH et al. 2003, BAUCH et al. 2005). Sea-ice formation can occur repetitively, especially in flaw polynyas, which are kept open by offshore winds and produce large amounts of sea-ice (BAREISS et al. 2005, ZAKHAROV 1997) and thereby release brine waters into the water column.

In agreement with the general movement of water from west to east along the Eurasian continental slope (NEWTON et al. 2008) higher salinity bottom waters of ~32 to 32.5 are generally advected from west to east in the Laptev Sea (BAUCH et al. 2010). This advected water is considerably higher in salinity compared to brine enriched bottom water at ~30 salinity. Even though sea-ice formation releases brines to the water column it has to be kept in mind that wind-driven polynya-openings and subsequent sea-ice formation events on a shallow shelf may lead to a freshening of bottom waters (Fig. 10). The initial bottom salinity decreases when predominantly wind-driven vertical mixing occurs between the still relatively fresh surface and the saltier bottom waters (Fig. 10). As brine-enriched waters did not dominate the bottom layer in summer 2007 but were found in the surface layer instead (BAUCH et al. 2010) the Laptev Sea data from 2007 shows a discontinuity at a higher salinity of about 32 (see Fig. 8).

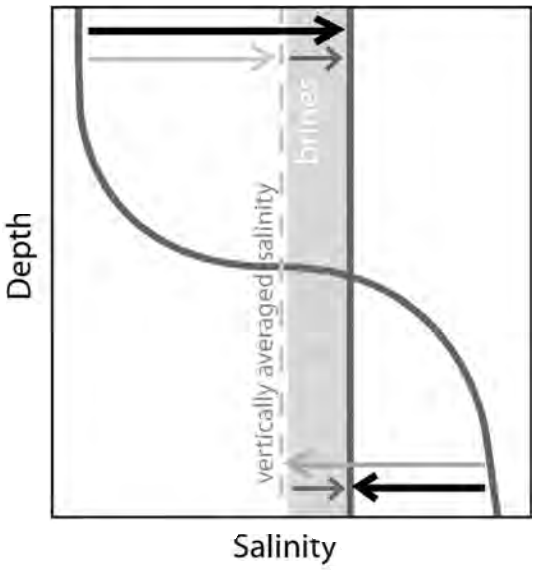

Fig. 10: Schematic drawing of a salinity profile transformed by a predominantly wind driven polynya. The typical salinity structure of the water column on the Arctic shelves with a distinct low salinity surface layer and a high salinity bottom layer (grey curve) is transformed into a uniform profile at the average salinity of the initial water column (light grey stippled line and arrows) increased by the amount of brines released to the water column by sea-ice formation (dark grey line and arrows). As a result (black arrows) salinity increases in the surface layer and decreases in the bottom layer when the effect of wind stress exceeds the effect of brine release.

Abb. 10: Schema zur Veränderung eines Salzgehaltprofils in einer überwiegend windgesteuerten Polynya. Die typische Salzgehaltsstruktur der Wassersäule auf den arktischen Schelfgebieten mit einer niedrig salinen Oberflächenschicht und einer hoch salinen Bodenschicht (graue Kurve) wird zu einer einheizlichen Salinität transformier bei einem Salzgehalt, der durch den Mittelwert der ursprünglichen Schichtung (hellgrau gestrichelte Linie und Pfeile), erhöht von den durch Meereisbildung in die Wassersäule abgegeben Salzlaken (Brines) (dunkelgraue Linie und Pfeile), bestimmt wird. Im Endeffekt (schwarze Pfeile) wird der Salzgehalt der Oberflächenschicht erhöht und der Salzgehalt der Bodenschicht verringert.

Exchange of waters at St. Anna Trough (Kara Sea)

The branch of Atlantic Water flowing across the Barents Sea enters the Arctic Ocean at St. Anna Trough. This region is generally considered to be a region of exchange between the shelf area and the Arctic Ocean interior (Schauer et al. 2002, RUDELS et al. 2004). Data from stations located along the Kara Sea continental slope at about 81 °N (ARK-XII; Figs. 6 and 7) all have higher salinities, indicating that there is no direct import of waters to the southern Kara Sea at 30 salinity. This finding also implies that there is no direct export of southern Kara Sea bottom waters into the Arctic Ocean halocline within the ARK-XII 1996 summer observations. The stations from the western slope of the St. Anna Trough (open circles in Fig. 6) have higher isotope values (at constant salinity) than those from the eastern slope (closed dots in Fig. 6). As the station data further to the east (crosses in Fig. 6) show no indication of further admixture of waters with low $\partial^{18}O$ value this documents an admixture of waters with low $\partial^{18}O$ values from the Kara or Barents Sea to the branch of Atlantic-derived waters flowing from south to north along the eastern slope of the St. Anna Trough (SCHAUER et al. 2002).

Exchange of water at the Laptev Sea continental margin

For data obtained at the Laptev Sea continental slope (Fig. 11) further analysis of the S and $\partial^{18}O$ data is conducted to derive a quantitative evaluation. Since the salinity and $\partial^{18}O$ are first order linearly correlated, the $\partial^{18}O$ data on a sectional distribution gives little additional information compared to salinity (see Fig. 11 for sections at ~125 °E taken in 1995). By applying a mass-balance calculation to the salinity and $\partial^{18}O$ data the deviation between salinity and $\partial^{18}O$ can be quantified

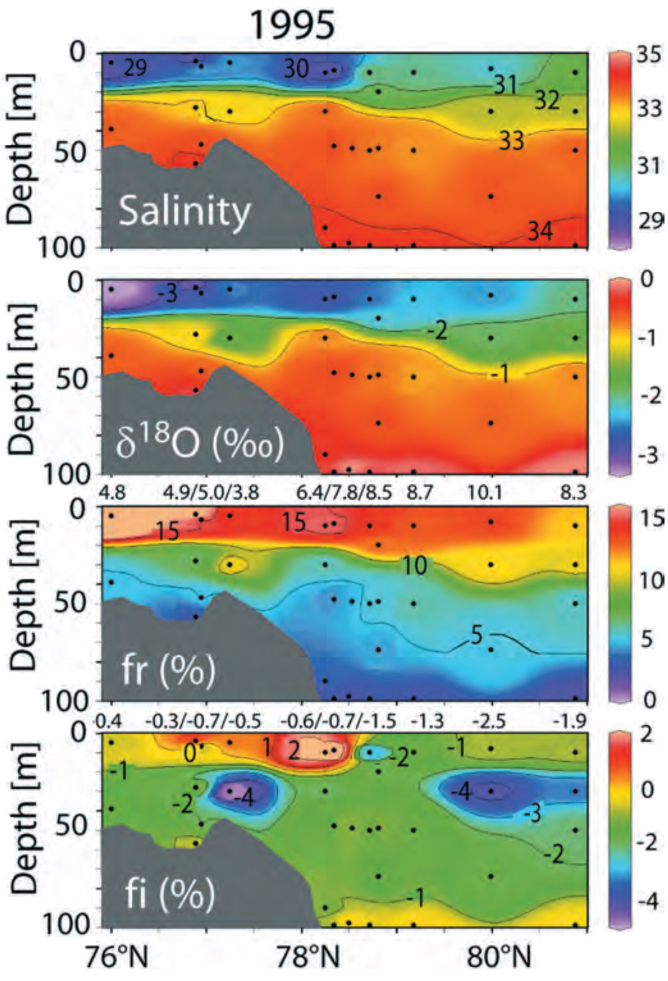

Fig. 11: Sections along about 125 °E of salinity and $\partial^{18}O$ as well as the calculated fractions of river water (fr) and sea-ice melt water (fi). Data are from summer 1995 with "offshore" atmospheric forcing (BAUCH et al. 2011). Inventory values of river water and sea-ice melt water (m) are shown on top of sections.

Abb. 11: Ozeanographischer Schnitt senkrecht zur Schelfkante der Laptewsee bei etwa 125 °E. Dargestellt sind Salzgehalte und $\partial^{18}O$ Werte und die daraus berechneten Fraktionen von Flusswasser (fr) und Meereisschmelzwasser (fi). Die dargestellten Daten des Sommers 1995 standen unter ablandig („offshore") atmosphärischem Antrieb. Die Budgetwerte von Flusswasser und Meereisschmelzwasser (m) der einzelnen Stationen stehen oberhalb der jeweiligen Abbildungsteile.

and the fractions of sea-ice melt water, river water and marine water of each water parcel can be calculated. The balance is governed by the following equations:

$$f_m + f_r + f_i = 1$$
$$f_m \cdot S_m + f_r \cdot S_r + f_i \cdot S_i = S_{meas}$$
$$f_m \cdot O_m + f_r \cdot O_r + f_i \cdot O_i = O_{meas}$$

Where f_m, f_r and f_i are the fractions of marine water, river-runoff and sea-ice melt water in a water parcel, and S_m, S_r, S_i, O_m, O_r and O_i are the corresponding salinities and $\partial^{18}O$ values. S_{meas} and O_{meas} are the measured salinity and $\partial^{18}O$ of the water samples. This concept was applied in several studies to the waters of the Arctic Ocean halocline (e.g. ÖSTLUND & HUT 1984, BAUCH et al. 1995, MACDONALD et al. 1995, EKWURZEL et al. 2001). Specific endmember values have to be chosen for the investigated area (see Tab. 2).

endmember	salinity	$\delta^{18}O$ (‰)
marine (f_{mar})	34.92	0.3
river (f_r)	0	- 20
sea-ice (f_i)	4	surface +2.6 or -7+2.6

Tab. 2: Endmember values used for mass-balance calculations.
Marine water: The choice of this parameter is most critical in terms of absolute values observed in the calculation for the freshwater fractions. However, the choice of this parameter does not influence the relative values between the fractions. We will calculate the fractions relative to Atlantic Inflow water with S = 34.92 and $\delta^{18}O$ = 0.3 ‰ which is the average value of the Atlantic layer in the southern Nansen Basin (ÖSTLUND & HUT 1984, BAUCH et al. 1995).
River-runoff: The average $\delta^{18}O$ of arctic runoff and precipitation is about -20 ‰.
Sea-ice melt water: The salinity of multi-year sea-ice is known to be about 4 (e.g. PFIRMAN et al. 1995). The $\delta^{18}O$ value of sea-ice is set to the measured $\delta^{18}O$ value of surface waters measured at the station multiplied with a fractionation factor of 1.0026 (MELLING & MOORE 1995). To avoid artefacts in the direct vicinity of the river mouth during summer surface values below -7 ‰ were substituted by -7 ‰ (BAUCH et al. 2010).

Tab. 2: Werte der Endglieder für die Massenbilanzberechnungen.
Meerwasser: Dieser Parameter bestimmt maßgeblich die absoluten Werte der berechneten Süßwasserfraktionen, wobei die relativen Werte jedoch unverändert bleiben. Die Fraktionen werden hier relativ zum Mittelwert des Atlantikwassers im südlichen Nansen-Becken mit S = 34.92 und $\delta^{18}O$ = 0.3 ‰ (ÖSTLUND & HUT 1984, BAUCH et al. 1995) berechnet.
Flusswasser: Mit -20 ‰ entspricht dies dem mittleren $\delta^{18}O$ Wert des arktischen Flusswassers und Niederschlags.
Meereisschmelzwasser: Der Salzgehalt von etwa 4 entspricht dem von mehrjährigem Eis (e.g. PFIRMAN et al. 1995). Für die $\delta^{18}O$-Signatur des Eises wird der Oberflächenwert der jeweiligen Station mit einem Fraktionierungsfaktor von 1.0026 (MELLING & MOORE 1995) multipliziert. Um Artefakte in der direkten Umgebung der Flussmündungen durch die sommerliche Flusswasserfahne zu vermeiden werden Oberflächenwerte kleiner als -7 ‰ durch den festen Wert -7 ‰ ersetzt (BAUCH et al. 2010).

Salinity, $\partial^{18}O$ data, and the results of the fraction calculations are presented in Figure 11 for data obtained in 1995. The fraction of river water and sea-ice melt water is given in % water volume for each water parcel; the fraction of the marine source is not shown and is the difference of the other fractions to 100 % (f_m (%) = 100 - f_r (%) - f_i (%)). Positive fractions of sea-ice reflect an addition of melt water, and negative fractions reflect a removal of water from the water column by sea-ice formation. At the surface river water fractions are between 15 to 10 % and sea-ice melt water fractions are variable with positive values up 2 % and negative values of about -1 %.

At the Laptev Sea margin at about 30 to 50 m water depth a pronounced signal is seen in the brine influence with about -4 % in sea-ice melt water fractions (Fig. 11). The origin of this brine-enriched water can be identified to originate at the southeastern Laptev Sea shelf. The brine-enriched waters on the Laptev Sea shelf fall on two different mixing lines in dependence on their salinities (see dashed mixing lines in Fig. 12). The waters at ~30 salinity contain the highest amount of brines (about 20 to 30 %) and are all bottom waters in the southern Laptev Sea below 20 m water depth (red squares in Fig. 12). These waters are all found within the region of the winter polynya (compare Fig. 3b). Since sea-ice is produced within the polynya at high rates and continuously throughout the winter, the polynya region is likely the production area for this brine-enriched bottom water (BEBW). But brine-enriched waters may also be formed during initial freeze-up beneath the land-fast ice in the southern Laptev Sea during October to December. A remnant of brine waters produced below the fast ice at considerable lower salinities is seen at two stations at salinities of about 27 and 28 (purple dots in Fig. 12) in a depression imbedded around a shallow bank in the southern Laptev Sea. But clearly the brine enriched bottom water at ~30 salinity is dominating the hydrography within the Laptev Sea as documented by the mixing lines in $\partial^{18}O$ / salinity data (Figs. 12 and Fig. 9).

Towards the north BEBW mixes with higher salinity water and is found either at the bottom (symbols with green numbers in Fig. 12) or at about 50 m water depth at the shelf break of the northeastern Laptev Sea (yellow triangles with orange and red numbers in Fig. 12). This indicates the entrainment of BEBW from the southern Laptev Sea into the Arctic Ocean halocline as also seen in the sectional data in 1995 at ~125 °E (Fig. 11). In the western Laptev Sea brine-enriched waters are found at the bottom (blue dots in Fig. 12) and at the shelf break at higher salinities and correspondingly deeper water depth.

The mixing scheme as suggested by the $\partial^{18}O$ / salinity data is compatible with an estuarine-like circulation on the Laptev Sea shelf (MACDONALD 2000, DMITRENKO et al. 2001) and is also in agreement with inter-annual variation in response to summer atmospheric forcing (DMITRENKO et al. 2005, GUAY et al. 2001). Inventories of river water (I_{riv}) and sea-ice melt water (I_{ice}) calculated for stations at the Laptev Sea continental slope for 1993, 1995, 2005 and 2006 (Fig. 13) show considerable inter-annual variation in correlation with summer atmospheric forcing (BAUCH et al. 2011). Nevertheless river inventories and sea-ice melt water inventories show a common pattern for all investigated years (Fig. 13). The increase of I_{riv} within the Eurasian Basin from the west to the east along the Laptev Sea continental slope is in accordance with the addition of river water from the Lena River at the Laptev Sea continental margin. The concurrent decrease of I_{ice} from positive values in the northwest of the Laptev Sea to increasingly negative inventory values towards the northeast documents the related addition of brine waters to the Arctic Ocean halocline from the eastern Laptev Sea (BAUCH et al. 2009).

The common pattern in river and sea-ice melt water inventories is found in all years despite the observed strong inter-annual variations. A correlation between river and sea-ice melt water patterns was also observed at the continental slope of the Beaufort shelf (YAMAMOTO-KAWAI et al. 2008). The correla-

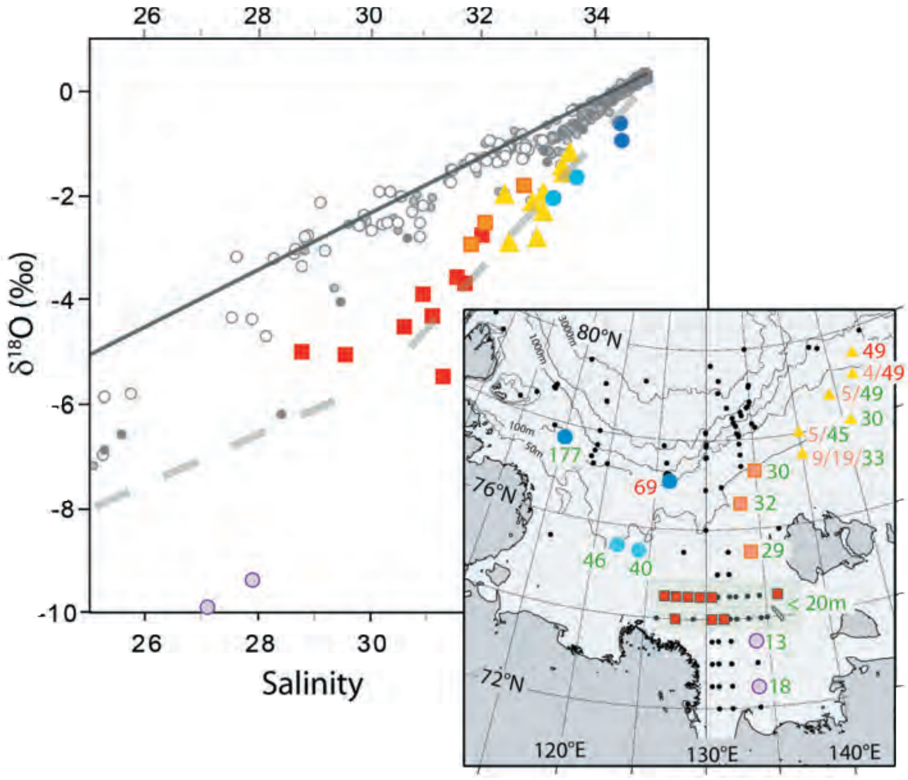

Fig. 12: Property plot of $\partial^{18}O$ versus salinity for data with salinities above 25 from summers 1993, 1994 and 1995. Data points on the light grey mixing line between Atlantic Water and brine-enriched bottom water were labelled according to their geographical distribution. The numbers given on the map next to the colour labelled positions give the depth of the brine-enriched waters in m. Green numbers are brine enriched waters found at bottom depth. Orange and red numbers are brine-enriched waters found above bottom depth. Stations in the south of the polynya region are shallower than 20 m and marked with a shaded green box.

Abb. 12: Die $\partial^{18}O$ Werte in Abhängigkeit von den Salzgehalten größer 25 für Sommerdaten 1993, 1994 und 1995 in der Laptev See. Die Werte entlang der Mischungslinie zwischen Atlantischem Wasser und meereisgeprägtem Bodenwasser sind entsprechend ihrer geographischen Lage gekennzeichnet. Die eingebettete Karte zeigt neben den jeweiligen Symbolen die Wassertiefe (m) der jeweiligen Probe. Die grünen Zahlen kennzeichnen Bodenwerte und die roten und orangen Zahlen kennzeichnen Meereis geprägtes Wasser oberhalb des Bodens. Stationen südlich der Polynya-Region sind flacher als 20 m und mit einem grünen Rechteck unterlegt.

tion of river and sea-ice melt water inventories at the Laptev Sea continental slope suggests that source region and transport mechanisms are closely linked over the relatively shallow Laptev Sea shelf. This is in agreement with the concept that both river water and sea-ice melt water (in this case negative fi) are transported by polynyas activity into the shelf's bottom layer and are released from the shelf by offshore wind forcing (BAUCH et al. 2009). The observed inter-annual differences in freshwater distributions (see also GUAY et al. 2001) are consistent with model results, which have demonstrated a potential for different freshwater spreading in correlation to the atmospheric forcing (JOHNSON & POLYAKOV 2001) With the calculated fractions we additionally derive quantitative information on the amount of river water and on the brine components contained in subsurface waters. The distribution of river water and sea-ice melt water fractions along the Laptev Sea continental slope documents the input of river water and a contribution of brine enriched waters from the Laptev Sea both east of 125 °E.

CONCLUSIONS

On all discussed Arctic shelf areas the net sea-ice production exceeds local sea-ice melting. The combined $\partial^{18}O$ / salinity summer data demonstrate that the influence of sea-ice production and sea-ice export is predominant within the Kara Sea, the Laptev Sea and the Beaufort Sea even during summer season when sea-ice is melting locally.

A brine enriched bottom water mass at about 30 salinity is observed in the S/$\partial^{18}O$ correlation of all shelves. Local bottom water is formed by sea-ice formation processes and remnants of these bottom water masses are found on all shelves during summer. Despite the differences in topography between the Kara, Laptev and Beaufort seas and considerably different salinity ranges brine-enriched bottom water with similar salinities of ~30 is found on all these shelves.

An admixture of river water to the Arctic Ocean is observed within St. Anna Trough at the Kara Sea continental margin. At the Laptev Sea continental margin an export of river water within the surface layer as well as an export of brine water below the surface layer at about 30-50 m water depth is observed. Both the export of river water and brine-enriched waters is controlled by summer atmospheric forcing and varies inter-annually in correlation with wind forcing accordingly.

The Arctic Ocean is a region most sensitive to global climatic change, which recently reflected most prominently in the decline of summer sea-ice coverage. In the climatically extreme summer 2007, with a so far unknown minimum in sea-ice cover, a significant change in brine production on the Laptev Sea shelf with an inverted distribution in the water column relative to previous observations was observed (BAUCH et al. 2010). A shift in the distribution of brine waters in the eastern Laptev Sea from the bottom layer to the surface layer alters the salinity range of waters exported into the Arctic Ocean (BAUCH et al. 2009). If this change in brine water distribution becomes more frequent or persists, it may have long-term consequences on the structure and stratification of the Arctic Ocean halocline. Therefore a further understanding of the processes and the exchange of water masses between the Arctic Ocean basin and the shelf areas is important in respect to halocline stability. A weaker halocline may impede sea-ice formation and enhance the ocean atmosphere heat flux thereby feeding back positively on Arctic climate warming.

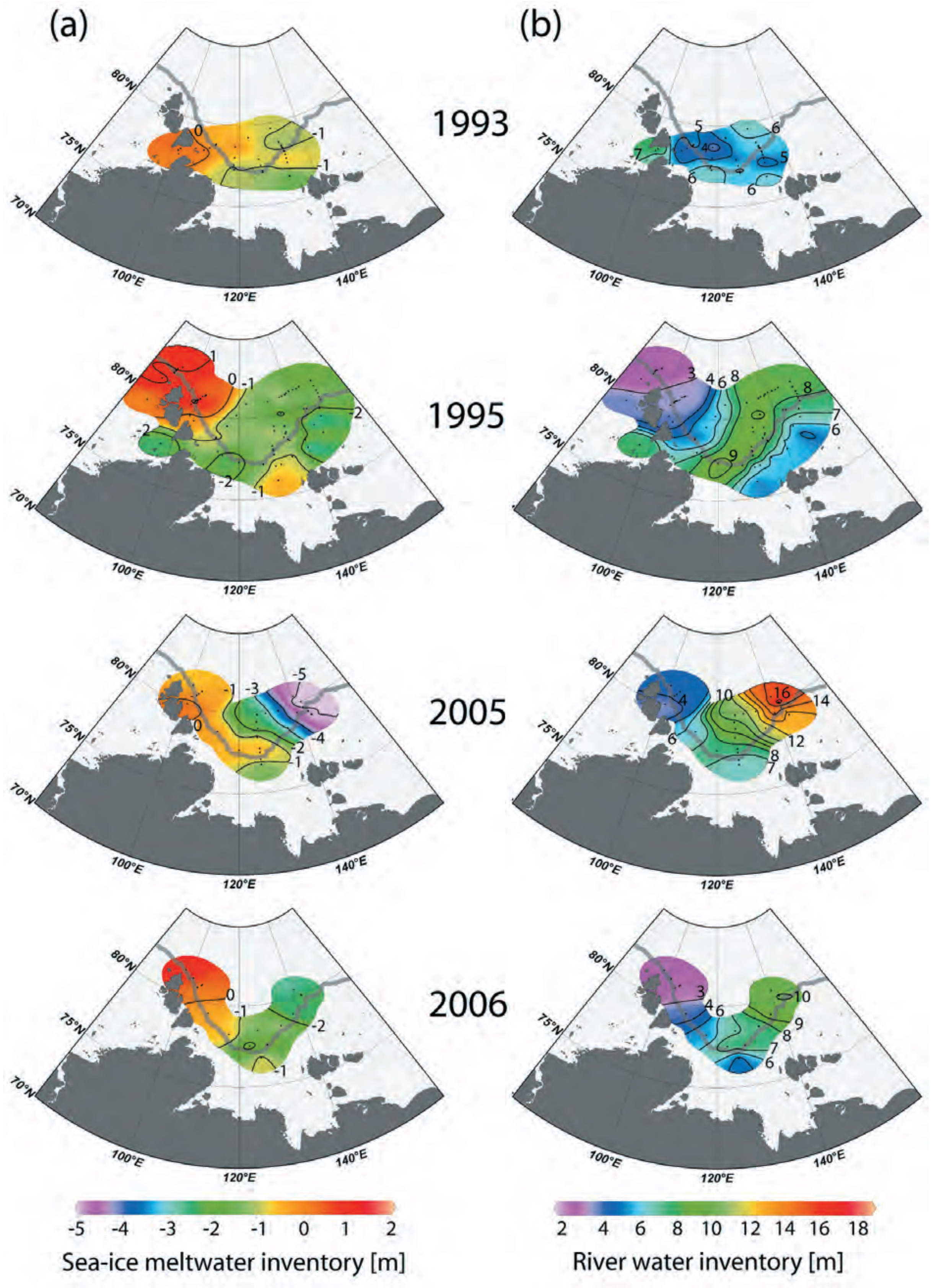

Fig. 13: Inventories of (a) sea-ice melt water and (b) river water. While "onshore" atmospheric forcing prevailed during summers 1993 and 2006, summers 1995 and 2005 were dominated by "offshore" atmospheric forcing (GUAY et al. 2001). The grey line indicates the 500 m isobath and the position of the continental slope.

Abb. 13: Budgetwerte von (a) Meereisschmelzwasser und (b) Flusswasser. Während der atmosphärische Antrieb in den Sommern 1993 und 2006 landwärts („onshore") geprägt war, waren die Sommer 1995 und 2005 ablandig („offshore") geprägt (GUAY et al. 2001). Die 500 m Tiefenlinie in Grau zeigt die Position des Kontinentalhanges.

ACKNOWLEDGMENTS

This work was part of the German-Russian cooperations "System Laptev Sea" and the "Otto-Schmidt-Laboratory for Polar and Marine Sciences" (OSL) funded by the German Ministry for Education and Research (BMBF), as well as by Roshydromet and the Russian Ministry of Education and Science. DB was additionally supported by the DFG under grant SP526/3. We thank all members of these projects for exceptional working conditions and extensive support during expeditions. We also thank the crew and the shipboard party of RV "Akademic Boris Petrov" for their help during the expeditions 1999, 2000 and 2001. We thank M. Frank and U. Schauer for collecting and providing data from ARK-XII. We thank all members of the NABOS project for exceptional working conditions and extensive support during expeditions. We are grateful for helpful and constructive comments from Leif Anderson and two anonymous reviewer. Plots were made with Ocean Data View (ODV) (SCHLITZER 2001) and Generic Mapping Tools (GMT) software (WESSEL & SMITH 1998).

References

Aagaard, K., Coachman, L. & Carmack, E (1981): On the halocline of the Arctic Ocean.- Deep-Sea Res. 28: 529-545.

Aagaard, K. & Carmack, E.C. (1989): The role of sea ice and other freshwater in the arctic circulation.- J. Geophys. Res. 94(C10): 14485-14498.

Anderson, L.G., Olsen, K. & Chierici, M. (1998): A carbon budget for the Arctic Ocean.- Global Biogeochem. Cycles 12(3): 455-465.

Bareiss, J. & Görgen, K. (2005): Spatial and temporal variability of sea ice in the Laptev Sea: Analyses and review of satellite passive-microwave data and model results, 1979 to 2002.- Global Planet. Change 48: 28-54. doi: 10.1016/j.gloplacha.2004.1012.1004.

Bauch, D. (1995): The distribution of $\partial^{18}O$ in the Arctic Ocean: Implications for the freshwater balance of the Halocline and the sources of deep and bottom waters.- Rep. Polar Res. 159: 1-144.

Bauch, D., Schlosser, P. & Fairbanks, R.F. (1995): Freshwater balance and the sources of deep and bottom waters in the Arctic Ocean inferred from the distribution of $H_2{}^{18}O$.- Progress Oceanogr. 35: 53-80.

Bauch, D., Carstens, J., Wefer, G. & Thiede, J. (2000): The imprint of anthropogenic CO_2 in the Arctic Ocean: evidence from planktonic $\partial^{13}C$ data from water column and sediment surfaces.- Deep-Sea Res. II 47: 1791-1808.

Bauch, D., Erlenkeuser, H., Stanovoy, V., Simstich, J. & Spielhagen, R.F. (2003): Freshwater distribution and brine waters in the southern Kara Sea in summer 1999 as depicted by $\partial^{18}O$ results.- In: R. Stein, D.K. Fütterer, E.M. Galimov & O.V. Stepanets (eds), Siberian River Run-off in the Kara Sea: Characterization, Quantification, Variability and Environmental Significance, Elsevier, Amsterdam, Proceedings in Marine Science 6: 73-90,

Bauch, D., Erlenkeuser, H. & Andersen, N. (2005): Water mass processes on Arctic shelves as revealed from ^{18}O of H_2O.- Global Planet. Change 48: 165-174. doi: 110.1016/j.gloplacha.2004.1012.1011.

Bauch, D., Dmitrenko, I.A., Wegner, C., Hölemann, J., Kirillov, S.A., Timokhov, L.A. & Kassens, H. (2009): Exchange of Laptev Sea and Arctic Ocean halocline waters in response to atmospheric forcing.- J. Geophys. Res. 114, C05008, doi: 10.1029/2008JC005062.

Bauch, D., Hölemann, J., Willmes, S., Gröger, M., Novikhin, A., Nikulina, A., Kassens, H. & Timokhov, L. (2010): Changes in distribution of brine waters on the Laptev Sea shelf in 2007.- J. Geophys. Res. 115, C11008, doi: 10.11029/12010JC006249.

Bauch, D., Gröger, M., Dmitrenko, I., Hölemann, J., Kirillov, S., Mackensen, A., Taldenkova, E. & Andersen, N. (2011): Atmospheric controlled freshwater water release at the Laptev Sea Continental marg.- Polar Res. 30: 5858, doi: 10.3402/polar.v5830i5850.5858.

Brezgunov, V.S., Debolskii, V.S.K., Mordasov, M.A., Nechaev, V.V. & Yakimova, T.V. (1980): Study of the conditions of formation of salinity of waters in the mouth regions of Arctic seas by means of natural stable oxygen isotopes.- Vodnye Resursy (in Russian) 2: 101-105.

Brezgunov, V.S., Debolskii, V.K., Nechaev, V.V., Ferronskii, V.I. & Yakimova, T.V. (1983): Characteristics of the formation of the oxygen isotope composition and salinity upon mixing of sea and river waters in the Barents and Kara Seas.- Water Resour. (Transl. of Vodnye Resursy, No. 4: 3-14, 1982), 9(4): 335-344.

Craig, H. (1961): Standard for reporting concentrations of Deuterium and Oxygen-18 in natural waters.- Science 133: 1833-1834.

Dansgaard, W. (1964): Stable isotopes in precipitation.- Tellus XVI: 436-468.

Dickson, B. (1999): All change in the Arctic.- Nature: 397, 389-391.

Dmitrenko, I.A., Hölemann, J., Kirillov, S.A., Berezovskaya, S.L., Eicken, H. & Kassens, H. (2001): Wind-forced currents as a linkage between the Laptev Sea (Siberia) and the Arctic Ocean.- Doklady Earth Sci. MAIK Nauka (in Russian) 377(1): 1-8.

Dmitrenko, I.A., Kirillov, S.A., Eicken, H. & Markova, N. (2005): Wind-driven summer surface hydrography of the eastern Siberian shelf.- Geophys. Res. Letters 32, L14613, doi: 14610.11029/12005GL023022.

Dmitrenko, I.A., Kirillov, S.A. & Tremblay, L.B. (2008): The long-term and inter-annual variability of summer fresh water storage over the eastern Siberian shelf: Implication for climatic change.- J. Geophys. Res. 113, C03007, doi: 10.01029/02007JC004304.

Ekwurzel, B., Schlosser, P., Mortlock, R. & Fairbanks, R. (2001): River runoff, sea-ice melt water, and Pacific water distribution and mean residence times in the Arctic Ocean.- J. Geophys. Res. 106(C5): 9075-9092.

Frank, M. (1996): Spurenstoffuntersuchungen zur Zirkulation im Eurasischen Becken des Nordpolarmeeres.- Diss. Univ. Heidelberg, 1-100.

Guay, C.K., Falkner, K.K., Muench, R.D., Mensch, M., Frank, M. & Bayer, R. (2001): Wind-driven transport pathways for Eurasian Arctic river discharge.- J. Geophys. Res. 106(C6), 11: 469-411,480.

Harms, I.H., Karcher, M.J. & Dethleff, D. (2000): Modelling Siberian river runoff - implications for contaminant transport in the Arctic Ocean.- J. Mar. Syst. 27: 95-115.

Harms, I., Hübner, U., Backhaus, J.O., Kulakov, M., Stanovoy, V., Stephanets, O.V., Kodina, L.A. & Schlitzer, R. (2003): Salt intrusions in Siberian River Estuaries – Observations and model experiments in Ob and Yenisey.- In: R. Stein, D.K. Fütterer, E.M. Galimov & O.V. Stepanets (eds), Siberian river run-off in the Kara Sea: Characterisation, Quantification, Variability and Environmental Significance, Elsevier, Amsterdam, Proceedings in Marine Science 6: 47-72,

Harms, I.H. & Karcher, M.J. (1999): Modelling the seasonal variability of hydrography and circulation in the Kara Sea.- J. Geophys. Res. 104(C6).

Johnson, M.A. & Polyakov, I. (2001): The Laptev Sea as a source for recent Arctic Ocean salinity changes, Geophysical Research Letters, 28(10), 2017-2020.

Létolle, R., Martin, J., Thomas, A., Gordeev, V., Gusarova, S. & Sidorov, I. (1993): ^{18}O abundance and dissolved silicate in the Lena delta and Laptev Sea (Russia).- Marine Chemistry 43: 47-64.

Macdonald, W., Paton, D., Carmack, E. & Omstedt, A. (1995): The freshwater budget and under-ice spreading of Mackenzie River water in the Canadian Beauford Sea based on salinity and $^{18}O/^{16}O$ measurements in water and ice.- J. Geophys. Res. 100: 895-919.

Macdonald, R.W. (2000): Arctic estuaries and ice: a positive-negative estuarine couple.- In: E. Lewis (ed), The freshwater budget of the Arctic Ocean, Kluwer Academic Press, Dordrecht, 383-407.

Melling, H. & Moore, R. (1995): Modification of halocline source waters during freezing on the Beauford Sea shelf: Evidence from oxygen isotopes and dissolved nutrients.- Cont. Shelf Res. 15: 89-113.

Mueller-Lupp, T., Erlenkeuser, H. & Bauch, H.A. (2003): Seasonal and inter-annual variability of Siberian river discharge in the Laptev Sea inferred from stable isotopes in modern bivalves.- Boreas 32: 292-303 doi: 10.1080/03009480310001984.

Newton, R., Schlosser, P., Martinson, D.G. & Maslowski, W. (2008): Freshwater distribution in the Arctic Ocean: Simulation with a high resolution model and model-data comparison.- J. Geophys. Res. 113 (C05024), doi: 10.1029/2007JC004111.

Östlund, H.G. & Grall, C. (1993): Arctic tritium: 1973-1991, Data Report 19, Univ. Miami, Rosenstiel School of Marine and Atmospheric Sci., Miami, Florida 33149.

Östlund, H. & Hut, G. (1984): Arctic Ocean water mass balance from isotope data.- J. Geophys. Res. 89(C4): 6373-6381.

Pfirman, S., Eiken, H., Bauch, D. & Weeks, W.F. (1995): The potential transport of pollutants by Arctic sea ice.- Sci. Total Environment 159: 129-146.

R-ArcticNET (2011): A Regional, Electronic, Hydrometric Data Network for Russia: Russian Daily Discharge Data from NSF-funded UCLA/UNH project.- http://www.r-arcticnet.sr.unh.edu/v4.0/index.html.

Rudels, B., Jones, E.P., Schauer, U. & Eriksson, P. (2004): Atlantic sources of the Arctic Ocean surface and halocline waters.- Polar Res. 23(2): 181-208.

Schauer, U., Loeng, H., Rudels, B., Ozhigin, V.K. & Dieck, W. (2002): Atlantic Water flow through the Barents and Kara Seas.- Deep-Sea Res. I 49: 2281-2298.

Schlitzer, R. (2001): Ocean Data View, http://www.awi-bremerhaven.de/GEO/ODV.

Shpaikher, O., Federova, Z.P. & Yankina, Z.S. (1972): Interanual variability of hydrological regime of the Siberian shelf seas in response to atmospheric processes (in Russian).- Proc. AARI 306: 5-17.

Stein, R. & Stepanets, O. (eds) (2000): Scientific Cruise Report of the Joint Russian-German Kara-Sea Expedition of RV "Akademik Boris Petrov" in

1999.- Rep. on Polar Res. 360: 1-141.

Stein, R. & Stepanets, O. (eds) (2001): The German-Russian Project on Siberian River Run-off (SIRRO): Scientific Cruise Report of the Kara-Sea Expedition "SIRRO 2000" of RV "Akademik Boris Petrov" and First Results.- Rep. Polar & Marine Res. 393: 1-287.

Stein, R. & Stepanets, O. (eds) (2002): Scientific Cruise Report of the Kara-Sea Expedition 2001 of RV "Akademik Boris Petrov": The German-Russian Project on Siberian River Run-off (SIRRO) and the EU Project "ESTABLISH".- Rep. Polar & Marine Rep. 419: 2-278.

Wessel, P. & Smith, W.H.F. (1998): New improved version of the Generic Mapping Tools released.- EOS Trans. Amer. Geopgys. Union 79: 579.

Yamamoto-Kawai, M., McLaughlin, F.A., Carmack, E.C., Nishino, S. & Shimada, K. (2008): Freshwater budget of the Canada Basin, Arctic Ocean, from salinity, $\partial^{18}O$, and nutrients.- J. Geophys. Res. 113 (C01007), doi:10.1029/2006JC003858.

Zakharov, V.F. (1997): Sea ice in the climate system.- Arctic Climate System Study, World Climate Research Programme, World Meteorological Organization, Geneva, WMO/TD 782, 1-80.